University of Groningen

Double-Layered Polyvinylpyrrolidone–Poly(Methyl Vinyl Ether-Alt-Maleic Acid) based Microneedles to Deliver Meloxicam

D'Amico, Carmine; Fontana, Flavia; El-Sayed, Nesma; Elbadri, Khalil; Correia, Alexandra; Rahikkala, Antti; Saarinen, Jukka; Shahbazi, Mohammad-Ali; Santos, Hélder A.

IMPORTANT NOTE: You are advised to consult the publisher's version (publisher's PDF) if you wish to cite from it. Please check the document version below.

Document Version
Publisher's PDF, also known as Version of record

Publication date:
2023

Link to publication in University of Groningen/UMCG research database

Double-Layered Polyvinylpyrrolidone–Poly(methyl vinyl ether-*alt*-maleic acid)-Based Microneedles to Deliver Meloxicam: An In Vitro, In Vivo, and Short-Term Stability Evaluation Study

Carmine D'Amico, Flavia Fontana,* Nesma El-Sayed, Khalil Elbadri, Alexandra Correia, Antti Rahikkala, Jukka Saarinen, Mohammad-Ali Shahbazi, and Hélder A. Santos*

This study aims to explore the use of polymeric microneedles (MNs) for the transdermal delivery of drugs, a noninvasive and convenient method that avoids first-pass metabolism and gastrointestinal complications. Specifically, a double-layered MN formulation is developed using polyvinylpyrrolidone and cross-linked poly(methyl vinyl ether-*alt*-maleic acid), comprising a dissolvable layer and a hydrogel-forming layer. Meloxicam serves as the model drug, and no organic solvents are employed in the manufacturing process to reduce toxicity. Coherent anti-Stokes Raman spectroscopy (CARS) is utilized to confirm that the manufacturing process does not alter the drug's physical properties. In vitro and ex vivo studies demonstrate that the double-layered MN formulation exhibits faster drug release in the first few hours, followed by a slower release. This results in extended bioavailability in vivo compared to the commercial oral formulation of meloxicam. Preliminary results indicate that the MN formulation is also effective in pain relief and inflammation reduction. The short-term stability of the MN formulation is also confirmed, including its mechanical properties, sustained skin permeability, drug physical properties and distribution within MNs using CARS microscopy. Overall, these results suggest that the double-layered MN formulation holds significant potential for transdermal drug delivery, offering a safer and more effective alternative to traditional oral administration.

1. Introduction

Transdermal drug delivery offers numerous advantages, including noninvasiveness, convenience, diminished risk of first-pass metabolism, and prevention of gastrointestinal complications.[1] The human skin, comprising the largest and outermost organ of the body, provides a convenient, selective, and noninvasive pathway for drug delivery.[2] While conventional needles enable drug delivery without the risk of enzymatic degradation or suboptimal absorption, they are associated with drawbacks such as pain, tissue damage, and needle phobia.[3] By contrast, transdermal patches circumvent many of these issues but are limited to drugs that can effectively permeate the skin.[4]

Microneedle (MN) patches offer a favorable combination of the benefits of traditional injections and transdermal patches in a user-friendly format, representing a highly promising modality for drug delivery.[1] However, despite significant progress, commercial products for

C. D'Amico, F. Fontana, N. El-Sayed, K. Elbadri, A. Correia, A. Rahikkala, J. Saarinen, H. A. Santos
Drug Research Program, Division of Pharmaceutical Chemistry and Technology, Faculty of Pharmacy
University of Helsinki
Helsinki 00014, Finland
E-mail: flavia.fontana@helsinki.fi; h.a.santos@umcg.nl

M.-A. Shahbazi, H. A. Santos
Department of Biomedical Engineering
University Medical Center Groningen
University of Groningen
Ant. Deusinglaan 1, Groningen 9713 AV, The Netherlands

M.-A. Shahbazi, H. A. Santos
W.J. Kolff Institute for Biomedical Engineering and Materials Science
University Medical Center Groningen
University of Groningen
Ant. Deusinglaan 1, Groningen 9713 AV, The Netherlands

**ADVANCED
SCIENCE NEWS**

www.advancedsciencenews.com

**ADVANCED
THERAPEUTICS**

www.advtherap.com

drug delivery applications are not yet available, possibly due to challenges in scaling up production and ensuring consistent quality control.[5–7]

While addressing these challenges, researchers have been focusing on biopolymeric MNs, which consist of microscale needles arranged in an array, can be self-administered, do not generate biohazardous sharps waste, and allow for the delivery of a diverse range of compounds. The latest form of MNs being researched are hydrogel-forming MNs, which are composed of swellable polymers or cross-linked hydrogels.[8] Unlike dissolving MNs, these MNs involve swelling rather than dissolving in the skin due to their hydrophilic nature.[9]

Bridging these formulations, our study introduces a double-layered MN patch that synergistically combines a dissolving layer and a hydrogel-forming layer, capitalizing on the benefits of both MN patch types. The outer dissolving layer expedites drug release, while the inner hydrogel-forming layer enhances drug retention and promotes a sustained release profile. This pioneering fusion heralds a novel approach to MN patch design, amplifying the potential of MN patches as a versatile and effective platform for transdermal drug delivery.

We chose meloxicam, a highly hydrophobic nonsteroidal anti-inflammatory drug, as the model drug to test the double-layered MN patch.[10] Previous studies have explored the use of meloxicam-loaded MNs,[11] yet our research is distinct in its pursuit of a double-layer formulation. A salient aspect of our methodology involves circumventing the use of organic solvents throughout the MN manufacturing process, making the process more environmentally friendly and cost-effective while minimizing potential toxicity. Choosing meloxicam was based on the fact that, while ≈40% of publications on dissolving and swellable MNs focus on small molecules, most of these studies use hydrophilic drugs due to their ease of incorporation into aqueous polymeric solutions.[12]

To create the double-layered MN patch, we employed polyvinylpyrrolidone (PVP) as the outer dissolving layer material and poly(methyl vinyl ether-co-maleic acid) (PMVE–MA) cross-linked with poly(ethylene glycol) diglycidyl ether (PEGDGE) for the hydrogel-forming layer.[13]

PVP has emerged as an exceptionally suitable material, thanks to its favorable attributes such as solubility in diverse solvents, biocompatibility, and capacity to enhance drug stability and solubility. Furthermore, PVP and other noncovalently aggregated polymers serve as cost-effective and intelligent drug delivery materials. Boasting desirable features like biostability, mechanical robustness, chemical resilience, low toxicity, and biocompatibility, PVP stands out as an exemplary excipient for drug delivery systems.[14] PVP MNs have demonstrated the ability to encapsulate various drugs within their polymeric matrix, and have shown stability after short-term stability studies.[15] PMVE–MA is a commonly used material in hydrogel-forming MNs and has been cross-linked with various materials as reported in literature.[16]

Although there have already been studies on double-layered or core–shell MN formulations, these studies focused on delivering insulin[17] or contraceptive hormones,[18] not on small hydrophobic molecules. The unique aspect of our MN formulation is its intended high drug concentration in the outermost layer, allowing for a high drug-loading dose and sustained drug release through the innermost layer. To the best of the authors' knowledge, this

is also the first time that PVP and PMVE–MA with this specific cross-linker are used in combination for a MN formulation.

When developing innovative pharmaceutical products, the solid-state properties of drugs in finished products assume a critical role. Potential modifications in the active pharmaceutical ingredient's crystalline state can substantially impact the drug's efficacy, stressing the necessity of assessing its crystal structure postfabrication.[19] In this regard, coherent anti-Stokes Raman scattering (CARS) microscopy introduces a cutting-edge technique for appraising the drug's crystalline state after MN fabrication, ensuring product quality.[20] Unlike traditional methods such as X-ray diffraction, CARS microscopy yields high-resolution images and imparts chemical information on the crystal structure without complex sample preparation.[21] As a nondestructive method, CARS microscopy facilitates real-time in situ imaging, thereby proving indispensable for examining the crystal structure of pharmaceuticals like meloxicam encapsulated within MN patches.[22]

Upon formulating meloxicam in a double-layered MN patch and assessing its critical attributes in terms of morphology, drug loading and status, and structural integrity, we proceeded to investigate the in vitro release and skin permeability, as well as evaluated the bioavailability and efficacy through in vivo studies. Moreover, we showcased the short-term stability of the formulation, providing a comprehensive assessment of its performance and potential for further development.

2. Results and Discussion

2.1. MN Morphology

Cross-linked MNs (MxMNs) were manufactured using the mold casting technique, which involved a combination of vacuum and centrifugation.[21] We performed an assessment of core–shell structure formation within the MNs using confocal microscopy (see Figure S1 in the Supporting Information). In **Figure 1**A–D, we show the pyramid-shaped needle of the MNs, where the tips of MxMNs (Figure 1A,B) exhibit a rougher surface in comparison to drugless MNs (Figure 1C,D). The increased roughness is attributed to the high concentration of meloxicam present in the tip area, which is not soluble in water. We opted to work with a meloxicam suspension instead of organic solvents to avoid potential undesired reactions and solvent traces within the patch.[11] Therefore, our preparation method allows for the drug to be arranged on the surface of the MNs as particles rather than mixed with the polymer matrix. This approach enables us to achieve a relatively high concentration of meloxicam without the use of organic solvents, avoiding any potential toxic residue, as opposed to other studies.[11]

2.2. CARS Analysis

We used CARS microscopy analysis to determine whether the solid state of meloxicam changed during the MN manufacturing process. The fluorescence of meloxicam powder in the CH—stretching region (2700–3200 cm^{-1}) is so high that it could not be used for imaging. However, lower CARS shift regions showed a good signal, and a characteristic CARS spectrum[22] was
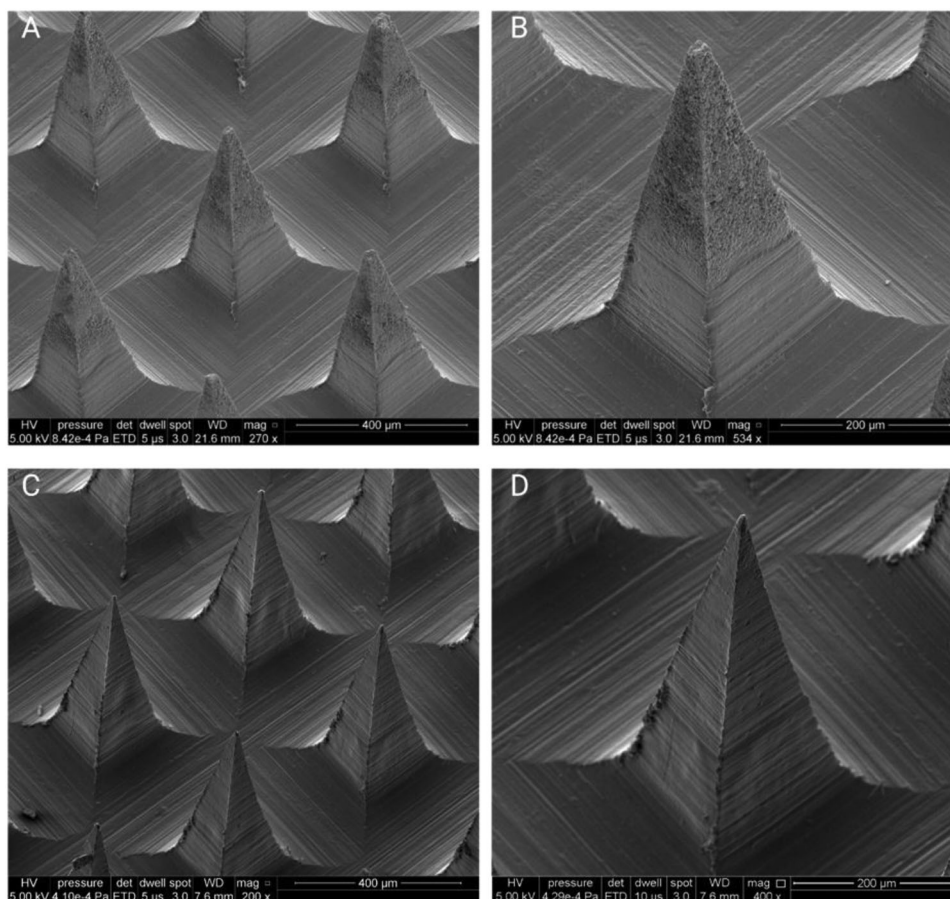
2300138 (2 of 10)

**ADVANCED
SCIENCE NEWS**

www.advancedsciencenews.com

**ADVANCED
THERAPEUTICS**

www.advtherap.com

Figure 1. SEM characterization of the MNs showing the uniform organization on the patch surface. A,B) Microscopy images show the presence of meloxicam in the form of concentrated particles at the tip of the MNs. C,D) Microscopy images show a smoother surface when the drug is not present in the MN formulation.

obtained between 1400 and 1800 cm^{-1} (**Figure 2**A). Furthermore, in the CARS spectrum area, both PVP and PMVE–MA showed no clear Raman peaks, making imaging our MN formulation possible. A comparison between two areas of the meloxicam powder (Figure 2B) and two CARS spectrum areas of the signal detected on the MNs (Figure 2C) can be observed. The detected spectra are superimposable, an essential indication regarding the preservation of the drug's crystalline form after the manufacturing process of the MNs. Figure 2D shows a 3D projection of the tip of one of the MNs, supporting the observations taken from the scanning electron microscope (SEM) images in Figure 1: meloxicam is localized predominantly on the tips and edges in the form of particles. To the best of our knowledge, this is the first time this kind of analysis has been performed on a MN formulation.

2.3. Mechanical Properties of MNs

To ensure successful use, MNs must be mechanically robust to withstand handling and insertion into the skin.[23] Previous research has shown that an average force of 30 N per MN array is applied during insertion by human volunteers.[24] In this study, we tested the mechanical properties of the cross-linked MNs for

4 h (MxMNs4h) formulation, which includes meloxicam, compared to MxMNs0h and a formulation without the drug.

Our results, presented in **Figure 3**A, demonstrate that the reduction in needle length after testing was $33 \pm 6\%$ for MxMNs4h and $33 \pm 5\%$ for MxMNs0h, indicating that cross-linking did not affect the mechanical strength of the MNs. However, the drugless MN formulation showed a reduction in length of only $26 \pm 5\%$, suggesting that adding meloxicam makes the MNs slightly more fragile than using polymers alone.

Our SEM and CARS images show a high drug concentration in the tips of the MNs, which may contribute to the slight reduction in mechanical strength. We also confirmed the results analyzing the deformation behavior of the formulation (Figure S2, Supporting Information). Overall, these findings suggest that while the addition of meloxicam may make the MNs slightly more fragile, the difference in mechanical strength is not statistically significant and is unlikely to affect their practical use.

We proceeded to test the insertion properties of the MN formulations on a skin-mimicking material made of eight layers of Parafilm M with a thickness of ≈1016 µm. As shown in Figure 3B, all MN formulations were successful in penetrating three to four layers of the material, indicating an insertion depth of 381–508 µm from the total 800 µm needle height.
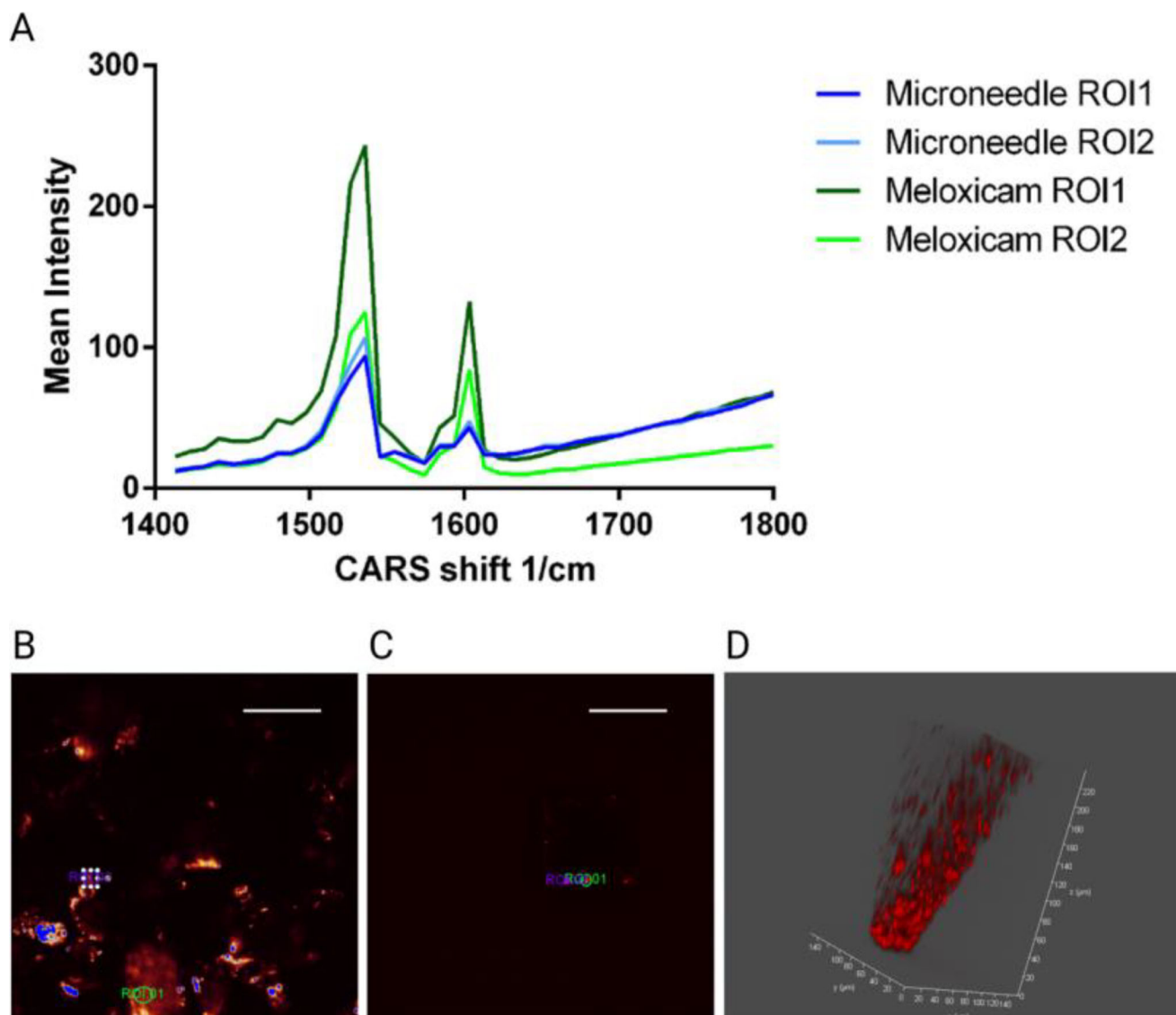
**ADVANCED
SCIENCE NEWS**

www.advancedsciencenews.com

**ADVANCED
THERAPEUTICS**

www.advtherap.com

Figure 2. CARS analysis to visualize meloxicam within the MN formulation. A) Raman peaks of meloxicam in the 1400–1800 cm^{-1} area were detected from two different areas of meloxicam powder and MxMNs. B) Epi-CARS image of meloxicam powder. Scale bar is 200 μm. C) Epi-CARS image of MxMNs. Scale bar is 200 μm. D) 3D projection of the tip of one of the MNs, to visualize meloxicam in particle form. For the images, we used the CARS shift at 1536 cm^{-1}.

To confirm the MNs' ability to penetrate skin layers, we examined the optical images of the holes left on the first to fourth Parafilm M layers. Our results revealed no significant differences in the ability of MNs to penetrate the material among the drugless MNs, MxMNs0h, and MxMNs4h formulations. We concluded that neither meloxicam incorporation nor the cross-linking reaction had any discernible influence on the ability of the MNs to penetrate the skin layer, which is a critical aspect of their practical use.

2.4. In Vitro Drug Release Study

To assess the efficacy of the cross-linking process, we conducted preliminary tests before investigating the drug release kinetics.

We immersed the polymeric films in water and found that only the film subjected to cross-linking conditions (exposure to 80 °C for 4 h) displayed significant swelling, while the other film dissolved. We analyzed the water absorption capacity (%WAC) over 24 h (Figure S3, Supporting Information) to further observe the polymer behavior. This robustly indicates successful cross-linking between PMVE–MA and PEGDGE.

To determine the drug loading degree, we dissolved the MN patches in 1× phosphate buffer saline (PBS) (pH 7.4) and analyzed the solution by high-performance liquid chromatography (HPLC) after 24 h. The average drug loading degree for each MN patch was 109 ± 11 μg, which translates to ≈1.09 μg of meloxicam in each needle of the 10 × 10 MN arrays we used. However, Pires et al.[25] worked with a 33 × 33 array, suggesting that the drug loading degree can potentially be increased with different molds.
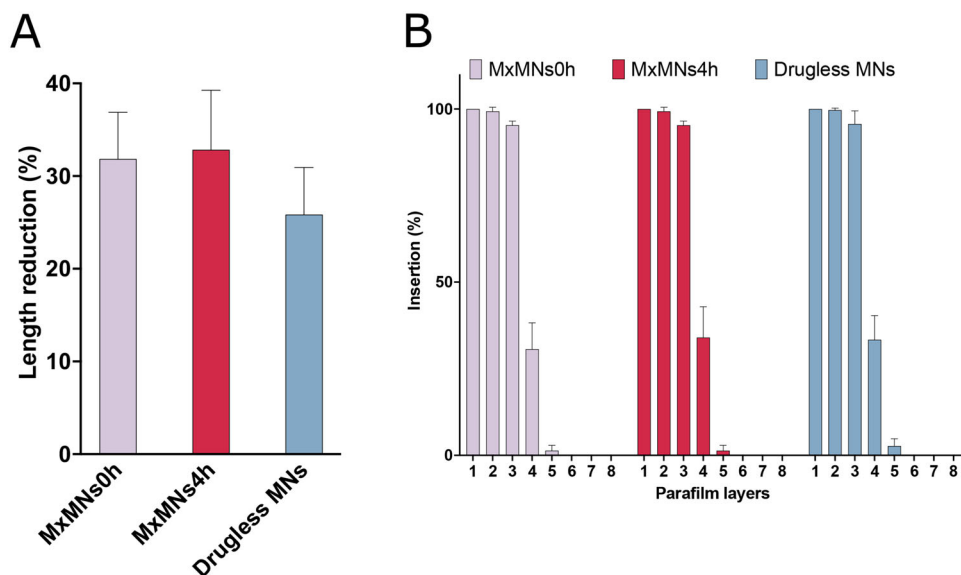
Figure 3. A) Length reduction of MNs after being pushed by the Texture Analyzer probe against the aluminum base. MNs were compressed against the flat aluminum base of the Texture Analyzer at a force of 30 N and a speed of 0.5 mm s^{-1} for 30 s. Pretest and post-test speeds were fixed at 1 mm s^{-1}, and a 0.05 N trigger force was set. B) Percentage of holes detected on the various Parafilm M layers during the skin piercing test.
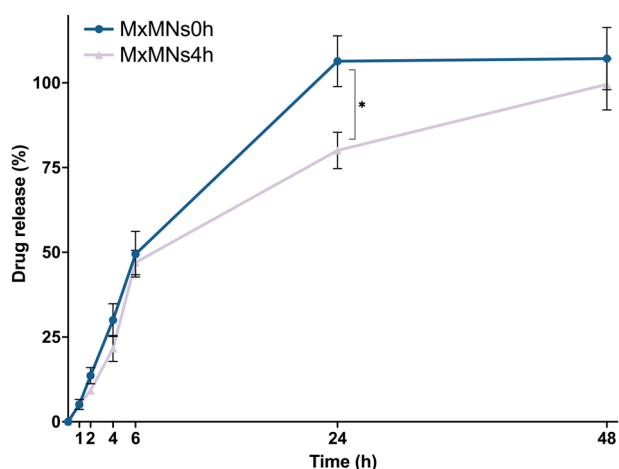

Figure 4. In vitro drug release for 48 h of the cross-linked and non-cross-linked MN formulations. The release experiments were conducted using 1× PBS (pH 7.4) as release medium, at 37 °C.
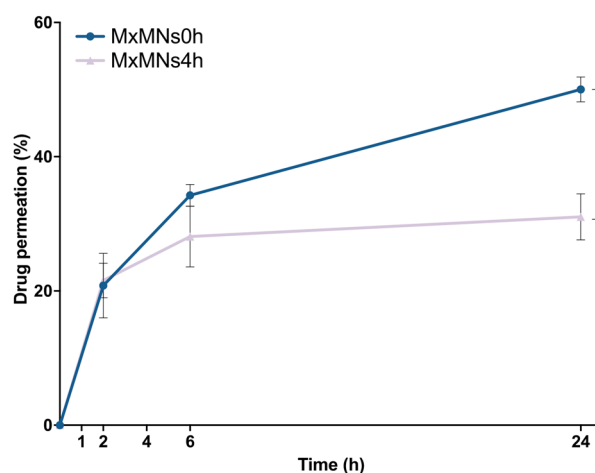

Figure 5. Skin permeability comparing cross-linked and non-cross-linked formulations. The release experiments were conducted using 1× PBS (pH 7.4) as release media at 37 °C.

As a control, we used the MxMNs0h formulation to examine the effects of inner layer cross-linking on the release profile of MxMNs4h in vitro. The release profiles are shown in **Figure 4**.

Both MN formulations exhibited comparable release patterns during the initial 6 h phase, attributable to the shared presence of a PVP outer layer in both configurations. During this period, ≈50% of the drug was released from each formulation. However, a marked distinction in the release rates emerged after 24 h. The un-cross-linked MN formulation, MxMNs0h, achieved complete meloxicam release, whereas MxMNs4h only released around 80% of the drug content. This divergence implies that PMVE–MA and PEGDGE underwent cross-linking in MxMNs4h's inner layer, culminating in a more finely tuned release profile. This profile is characterized by an accelerated initial release during the

first 6 h and a sustained, gradual release over the subsequent 48 h period.

Compared to another study, where 100% of in vitro meloxicam release was achieved in less than 1 h,[26] our formulation achieved a more desirable release profile.

2.5. Skin Permeation Study

After evaluating the insertion properties of the mimic-skin model, we proceeded to insert the MNs into porcine skin. **Figure 5** displays the ex vivo permeation profiles of meloxicam across porcine skin over a 24 h period using the MxMNs0h and MxMNs4h formulations. The majority of the drug was detected in the viable skin, while only a small amount (always
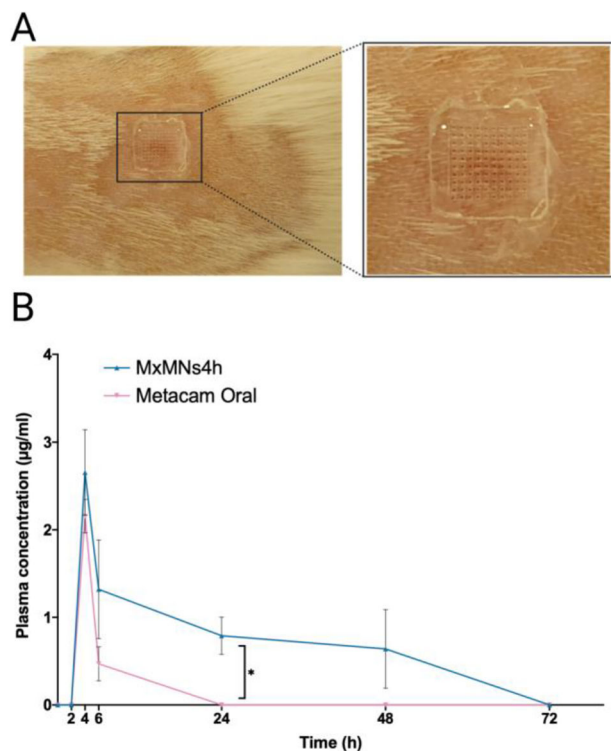
**ADVANCED
SCIENCE NEWS**

www.advancedsciencenews.com

**ADVANCED
THERAPEUTICS**

www.advtherap.com

Figure 6. A) MxMNs are inserted on the back of a rat. B) Plasma concentration comparing MxMNs4h and oral formulation of Metacam given to the animal. Each treatment group was composed of 7 animals, 4 males and 3 females.

less than 5 µg) reached the receptor cells, which was expected due to meloxicam's hydrophobic properties. As noted in previous studies,[27] it is advantageous if a more significant amount of the drug is deposited in the skin since this has the potential to make the drug more effective for a more extended period while simplifying dosing regimens. The MxMNs4h formulation exhibited a more gradual drug release rate, as already evidenced by the in vitro release study. At the 24 h mark, just 31% of meloxicam was detected in the viable skin and receptor cells when utilizing the MxMNs4h formulation, in contrast to the un-cross-linked MxMNs0h formulation, which displayed ≈50% meloxicam detection after the same duration. Consequently, we deduce that the MxMNs4h formulation provides a superior level of control over meloxicam release.

2.6. In Vivo Study

After successfully administering MNs to rats (**Figure 6**A), we measured the plasma concentration of meloxicam at various time points and calculated the bioavailability by measuring the area under the curve. The results in Figure 6B show that the bioavailability of meloxicam using MxMNs4h was $50 \pm 10\%$, with the highest concentration reached after 4 h, and a constant blood concentration maintained until 48 h. By avoiding administration of Metacam via oral gavage, the amount of drug the rats ingested was limited, resulting in a bioavailability of less than 10% of the intended dosage. The literature reports the oral bioavailability of

Metacam to be 98%,[28] although other studies report a range from 48% to 92%.[29] Orally administered meloxicam was undetected after 6 h. However, studies also report that when administered orally, meloxicam has a half-life of 7.7 h.[28] After applying the MxMNs4h formulation, the bioavailability of meloxicam was lower than the data reported for the commercially available oral formulation. Several factors may have contributed to this issue, such as possible partial insertion of the MNs into the rat's skin or the animal's poor compliance during the experiment. The animals sometimes removed the MN patch prematurely before the MNs detached from the base. Nonetheless, we observed a significantly longer half-life of the MN formulation than the oral counterpart.

In addition to the bioavailability study, we conducted preliminary studies to evaluate the anti-inflammatory and pain-relieving effects of the formulation. Specifically, we measured Arginase1 values in the blood (see Figure S4 in the Supporting Information) and performed the tail-flick test on animals (see Figure S5 in the Supporting Information). Although these initial results are promising, further investigations are required to assess the levels of other cytokines. Moreover, it would be valuable to extend the evaluation of the tail-flick test to different models, as we only performed the experiment on healthy animals, due to laboratory animal center restrictions.

Finally, in order to comprehensively evaluate the health status of the animals at the conclusion of our study, we performed additional assessments beyond those directly related to our primary objectives. Specifically, in addition to evaluating the efficacy of our formulation, we also measured changes in spleen weight and levels of macrophages and T-cells (Figures S6–S8, Supporting Information). These additional assessments provide a more complete understanding of the effects of our treatment on the animals, as well as any potential systemic effects that could impact the validity of our results. After euthanizing the animals, we found no significant changes in spleen weight or levels of macrophages and T-cells, indicating that our formulation had no deleterious effects on the overall health of the animals.

2.7. MN Short-Term Stability

To assess the short-term stability of the MN formulation, we conducted further experiments comparing critical attributes of freshly prepared MNs with those stored for 60 days under different conditions. Specifically, we examined the impact of storage on the drug's skin permeability, and compared the results to the freshly prepared MNs. Notably, we observed that the drug permeation profiles were almost identical between the two formulations, with no statistically significant differences ($p > 0.26$) observed for MNs stored under dry conditions or those kept at room temperature (RT) (see **Figure 7**).

We also compared the mechanical properties and piercing abilities of the MN formulations after storage. Although a slight increase in length reduction was observed in the MNs stored under dry conditions, there were no statistically significant differences between the fresh and stored formulations (all p-values > 0.9) (Figure S9A, Supporting Information). Similarly, the piercing properties of the needles showed no significant differences (Figure S9B, Supporting Information).
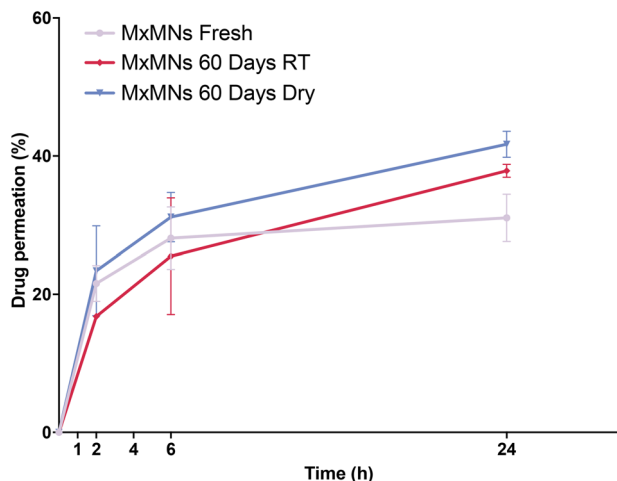
**ADVANCED
SCIENCE NEWS**

www.advancedsciencenews.com

**ADVANCED
THERAPEUTICS**

www.advtherap.com

Figure 7. Skin permeability for 24 h comparing the fresh formulation of MxMNs4h with samples stored at room temperature or in dry conditions for 60 days. The release experiments were conducted using 1× PBS (pH 7.4) as release media at 37 °C.

In the final analysis, we sought to investigate the polymorphism of meloxicam, a topic of significant interest since it exists in two distinct crystalline forms: a zwitterionic form and an enolic form.[30] Form I, the enolic form, is preferred for pharmaceutical preparations. Using CARS microscopy, we verified that the polymorph form of meloxicam remained unchanged after loading into the MNs. Additionally, no differences were observed in the drug signal between fresh and stored MNs (**Figure 8**). Our results indicate that under the conditions used to test short-term stability, our formulation maintained both its physical and mechanical properties and the sustained drug release observed in the freshly prepared MN formulation.

3. Conclusion

In this study, we fabricated a MN patch by combining PVP and cross-linked PMVE–MA to combine the characteristics of dissolvable MNs with those of hydrogel-forming MNs. Meloxicam was used as a model drug, and its manufacturing process within the MNs avoided using organic solvents, making the process greener and less toxic in the final formulation. SEM images showed the accumulation of the drug in the form of particles on the tips of the MNs, which was also confirmed by CARS analysis, thus confirming that meloxicam did not change its crystalline form during the manufacturing process of the MNs. The in vitro drug release studies showed the presence of two different types of release profiles related to the different compositions of the two MN layers: the outer layer, consisting of PVP, had a faster release, while the inner layer, consisting of PMVE–MA cross-linked with PEGDGE, showed a slower and more sustained release of meloxicam. Similar behavior was also observed in the pig skin permeability experiment. The study showed that, with this MN formulation, a prolonged plasma concentration of meloxicam was achieved compared to the corresponding oral formulation. Although we only performed a preliminary in vivo analysis, we also found positive results in pain management and treating inflammation in ani-

mals. Furthermore, the MN formulation was stable even after 60 days stored in both dry conditions and at room temperature.

Overall, our study confirms the potential of combining polymers with different properties within the same MN formulation to deliver small, highly hydrophobic drug molecules, which can impact the administration of these and similar compounds in a clinical setting.

4. Experimental Section

Analytical Method for Meloxicam: The content of meloxicam (molecular weight: 351.40 g mol^{-1}, Thermo Fisher, USA) in the samples was quantified with HPLC (1260 Infinity, Agilent Technologies, USA), using a Discovery C$_{18}$ column (Supelco, 5 µm, Sigma-Aldrich, USA) kept at +40 °C, with a flow composed of 0.2% phosphoric acid:methanol (40:60, v/v-%), a flow rate of 1 mL min^{-1}, injection volume of 10 µL, and a retention time of 5.1 min, according to a calibration curve of meloxicam in PBS (pH 7.4).

Casting Suspension Preparation: A small porcelain mortar was used with an outside diameter of 150 mm to mix 50 mg of meloxicam with 0.3 mL of 6 w/v-% hydroxyethyl cellulose, repeating the procedure until a smooth paste free of agglomerates was obtained. 4 mL of water was then slowly added while stirring to form a suspension with a meloxicam concentration of 11.6 mg mL^{-1}. For the two layers of the MNs, separate 30% w/v polymer solutions of PVP (wt ≈360 000, Sigma-Aldrich, USA) in ultrapure water and PMVE–MA (wt ≈1 980 000, Sigma-Aldrich, USA) in Milli-Q Water were prepared. The outer layer casting suspension was prepared by mixing the meloxicam suspension and PVP solution at a 3:1 ratio, resulting in an 8.7 mg mL^{-1} meloxicam concentration and a 7.5% w/v PVP concentration. The inner layer casting suspension was prepared by mixing equal parts of the meloxicam suspension and PMVE–MA solution, resulting in a meloxicam concentration of 5.8 mg mL^{-1} and a PMVE–MA concentration of 15%. Finally, 0.006% v/v PEGDGE (wt ≈500, Sigma-Aldrich, USA) was added as a cross-linker. The %WAC of the cross-linked polymer was calculated using the Equation (1)

$$\%WAC = \frac{m_t - m_0}{m_0} \times 100 \tag{1}$$

where m_t is the weight of the swollen sample at time t and m_0 is the initial weight of the dry sample.

Design and Fabrication of the Double-Layer MN Patch: 30 µL of suspension was added to the polydimethylsiloxane mold templates, featuring dimensions of 800 µm height, 200 µm base, and 500 µm pitch. Using these mold templates, MNs were arranged in a 10 × 10 array with a pyramidal shape. After pouring the suspension, the molds were placed in a vacuum chamber for 2 h, excess suspension was removed, and the process was repeated. The molds were then centrifuged for 10 min at 3000 rpm (1811*g*) to concentrate the suspension at the bottom and excess polymer was removed. The MNs were left to dry overnight at room temperature.

For the inner layer, a mixture of meloxicam, PMVE–MA, and PEGDGE was utilized. The same steps as for the first layer were followed and the MNs inside the molds were allowed to dry overnight at room temperature. As a final step, a 30% PVP solution was added to form the patch's base, which was then transferred to an oven at 80 °C for 4 h to cross-link the PMVE–MA and PEGDGE. MxMNs4h was compared with a formulation containing the same polymer composition that did not undergo the cross-linking reaction (MxMNs0h) throughout the study.

Scanning Electron Microscopy: The morphology of MN surfaces was observed by SEM (Ultra Plus, Zeiss, Germany). Prior to imaging, all samples were coated with palladium and then imaged at an accelerating voltage of 10 kV.

Coherent Anti-Stokes Raman Spectroscopy: The CARS microscopy system was described in detail elsewhere.[31] A Leica TCS SP8 CARS microscope (Leica Microsystems GmbH, Wetzlar, Germany) was used. Samples were placed on a coverslip No. 1.5 and measurements were done at RT. Using an HyD detector, CARS spectra were measured between 1413
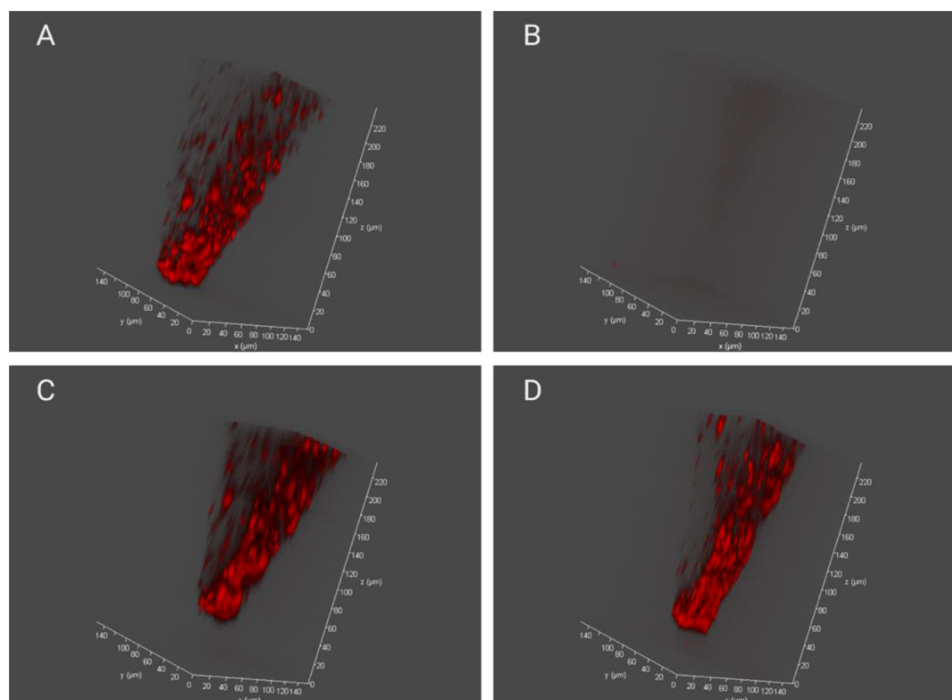
**ADVANCED
SCIENCE NEWS**

www.advancedsciencenews.com

**ADVANCED
THERAPEUTICS**

www.advtherap.com

Figure 8. MN tip 3D projections obtained by CARS imaging, using the CARS shift at 1536 cm^{-1}. A) Epi-CARS image of fresh MxMNs4h MNs. B) Epi-CARS image of drugless MNs. C) Epi-CARS image of MxMNs4h stored for 60 days at room temperature. D) Epi-CARS image of MxMNs4h stored for 60 days in dry conditions.

and 1800 cm^{-1} by systematically tuning the wavelength of the pump laser 33 times (893.3–925.3 nm). The second-order nonlinear spectra containing the sum frequency generation (SFG) and second harmonic generation (SHG) signals were recorded in the range 400–700 nm by exciting the sample with the Stokes wavelength of 1064.5 nm and a pump wavelength of 915 nm. The positions of the peaks and the absence of a broader background signal were used to confirm that the detected signal originated from crystalline material (and, therefore, meloxicam).

Stability Study: The study investigated the short-term stability of MxMNs4h with regard to mechanical properties, insertion properties, and skin permeability for a period of 60 days. Two different conditions were tested to assess stability: the samples were kept at room temperature (20 ± 2 °C) and relative humidity (RH) of 50%, or in dry conditions (+40 ± 2 °C), 20% RH, which was in line with World Health Organization requirements for stability studies of pharmaceuticals intended for specific markets.[32]

Mechanical and Insertion Tests: The mechanical properties of the MNs were evaluated using a Texture Analyzer (CT3, Brookfield, Canada) in compression mode. The initial height of MNs was measured using an optical microscope (EVOS XL, Invitrogen, USA). MNs were attached by double-sided adhesive tape to the movable cylindrical probe of the Texture Analyzer. MNs were compressed against the flat aluminum base of the Texture Analyzer at a force of 30 N and a speed of 0.5 mm s^{-1} for 30 s. Pretest and post-test speeds were fixed at 1 mm s^{-1}, and a 0.05 N trigger force was set. The MNs were imaged once again with an optical microscope. MN heights were determined using the optical microscope. The percentage (%) height reduction of height after applying the axial compression load was determined using Equation (2)

$$\%\text{Height reduction} = \frac{\text{original height} - \text{new height}}{\text{original height}} \times 100 \qquad (2)$$

MN piercing ability was assessed with Parafilm M (Amcor, USA) for the insertion properties of MNs. For MN penetration studies, Parafilm M

layers were previously validated as skin simulants.[33] The initial height of MNs was measured using the optical microscope. Later, the Parafilm M sheet was folded into an eight-layer film (≈1 mm thickness). Subsequently, MNs were attached to the movable probe of the Texture Analyzer. The probe was lowered onto the folded Parafilm M at a speed of 0.5 mm s^{-1}, using a defined force of 30 N applied for 30 s. Then, the Parafilm M sheet was unfolded, and, subsequently, the number of holes generated in each layer was determined using the optical microscope (EVOS XL, Invitrogen, USA).

In Vitro Drug Release Study: In vitro release experiments were conducted with the help of double-sided tape on the back of the base. A single MN was wrapped inside a filter membrane of 0.4 µm (Whatman polycarbonate membranes, Sigma-Aldrich). In a glass vial, each wrapped patch was dipped into 10 mL of 1× PBS (pH 7.4) at +37 °C. The solution was stirred at 120 rpm and kept in an oven at +37 °C to maintain a constant temperature. At 1, 2, 4, 6, 24, and 48 h, after placing the MNs in the solution, 500 µL of the release solution was collected from each vial and replaced with 500 µL of fresh PBS buffer (pH 7.4) at +37 °C. The content of meloxicam in the samples was quantified with HPLC using the method previously described.

In Vitro Skin Permeation Study: Franz diffusion cells were used for the study of permeability. Pig skin was used as a model membrane in ex vivo studies. The skin was sandwiched between a donor and an acceptor compartment (chamber), leaving a diffusion area of 0.64 cm^2. The media in the acceptor chamber was 12 mL of 1× PBS (pH 7.4). The skin was kept at 37 °C using a circulating water bath in the jacket of the Franz cells. MNs were inserted in the pig skin with a Texture Analyzer, as described above, to ensure an even penetration into the skin. The skin was then placed between the donor and the acceptor chamber. The samples were collected at 0, 2, 6, and 24 h after insertion of the microneedles in the skin from the acceptor chamber. At each time point, the skin was removed from the Franz cells, cleaned from MN leftovers left with adhesive tape, cut into small pieces, and added to 10 mL of methanol to extract the drug permeated in the viable skin. HPLC

**ADVANCED
SCIENCE NEWS**

www.advancedsciencenews.com

**ADVANCED
THERAPEUTICS**

www.advtherap.com

was used to analyze all the samples according to the method described previously.

In Vivo Efficacy in a Tail Flick Test: All the animal experiments were approved by the Finnish Regional State Administrative Agency with license no. ESAVI/26327/2021 – Project 4. Briefly, the animals were housed in the Laboratory Animal Center of the University of Helsinki, Finland. Male (225–249 g) and female (150–174 g) Wistar rats (RccHan:WIST, Envigo, The Netherlands) were housed in groups of 3 animals per cage. The animals were fed a standard rodent diet and housed with 12 h light/dark cycles. All the animals were trained to eat Nutella (Ferrero, Italy) with sterile water at 22 °C in the week before the experiment. Each treatment group, Metacam oral administration mixed with Nutella, or F1, administered 6 or 24 h before the test, was composed of 6 animals, 3 males and 3 females. On the day of the test, the tail of the animals was immersed in sterile water at +52 °C and the time before the animal flicked the tail was measured. The detailed protocol for this study is reported in Supporting Information.

In Vivo Efficacy in a Systemic Inflammation Model: Each treatment group, sterile PBS intraperitoneally (IP), lipopolysaccharides (LPS, 0.1 µg kg^{-1}) IP, LPS (0.1 µg kg^{-1}) IP + Metacam oral administration mixed with Nutella, or LPS (0.1 µg kg^{-1}) IP + F1 was composed of 6 animals: 3 males and 3 females. All the animals were shaved with a razor one day before the experiment, followed by hair removal cream on the back. The shaven areas were then cleaned with a glycerol disinfectant to prevent skin inflammation. On day 0, each animal was anesthetized with isoflurane (2%) and injected IP with PBS or LPS according to the group. The skin of the rats receiving the MNs was slightly wetted with sterile PBS, and the MNs were then gently placed on the skin and pressed with a finger, followed by 5 rounds of MN applicator (Micropoint Technologies Pte Ltd., Singapore). The patch was then kept in place with two pieces of adhesive bandages. Each animal was then moved to a single cage for recovery. Once the animals woke from the anesthesia, Nutella or Nutella mixed with Metacam (0.5 mg mL^{-1}, oral formulation for cats, Boehringer Ingelheim) was offered for the rats in the oral administration group. The animals were weighed daily.

Furthermore, blood was collected from vena saphena in 3 animals per group daily. On day 4, after the blood sampling, each animal was sacrificed by terminal isoflurane anesthesia, followed by cervical dislocation and collection of the spleen. Each spleen was washed twice with sterile PBS, weighted, and smashed into a single-cell suspension. The single-cell suspension was strained through a 40 µm strainer (431750, Corning, USA) and immediately used to analyze the immune cells or quantify the cytokines.

In Vivo Bioavailability: The Finnish Regional State Administrative Agency approved all the animal experiments with license no. ESAVI/26327/2021 – Project 2 and modification no. ESAVI/12581/2022. The animals were housed in the Laboratory Animal Center of the University of Helsinki, Finland. Male (250–274 g) and female (175–199 g) Wistar rats (RccHan:WIST, Envigo, The Netherlands) were housed in groups of 4 (male) or 3 (female) animals per cage. The animals were fed a standard rodent diet and housed with 12 h light/dark cycles. All the animals were trained to eat Nutella (Ferrero, Italy) the week before the experiment. Each treatment group (Metacam oral administration mixed with Nutella, or MNs 4 h) was composed of 7 animals, 4 males and 3 females. One day before the experiment, all the animals were shaved with a razor, followed by hair removal cream on the back and the hind paws to allow for easier access to vena saphena during blood sampling. The shaven areas were then cleaned with a glycerol disinfectant to prevent skin inflammation.

On day 0, each animal was anesthetized with isoflurane (2%). The skin of the rats receiving the MNs was slightly wetted with sterile PBS. The MN patches were then gently placed on the skin and pressed with a finger, followed by 5 rounds of MN applicator (Micropoint Technologies Pte Ltd., Singapore). The patch was then kept in place with two pieces of adhesive bandages. Each animal was then moved to a single cage for recovery. Once the animals woke from the anesthesia, Nutella or Nutella mixed with Metacam (0.5 mg mL^{-1}, oral formulation for cats, Boehringer Ingelheim) was given to the rats in the oral administration group. Blood samples (200 µL per sample) from the vena saphena were then collected at the following time points 2, 4, 6, 24, 48, 72, and 96 h in MiniCollect

Tubes 0.25 mL/0.5 mL K2EDTA (Greiner Bio One, USA). Blood samples were collected from 3 animals for each group at each time point. After the first 6 h, the animals were placed back in the group cages for the rest of the study.

Upon completion of the study, the animals were euthanized with CO_2, followed by cervical dislocation. The blood samples were spun at 3000 rpm (1811g) on an Eppendorf centrifuge for 10 min to separate the plasma from the other blood components. The plasma was then pipetted in low-retention Eppendorf. An equal amount of methanol (HPLC grade) was added to each Eppendorf, followed by extensive vortexing and centrifugation at 16.1g on an Eppendorf centrifuge for 10 min to precipitate plasma proteins. The clear supernatant was then transferred to 96-well plates (Nunc) and analyzed in HPLC using the method previously described. A linear calibration curve was obtained in plasma before analyzing the samples.

Statistical Analysis: All the data were analyzed with Prism 8 (Graph-Pad Software, USA). The difference was considered significant when the *p-value was <0.05. Ordinary one-way Analysis of Variance (ANOVA) followed by a Dunnett post hoc test, ordinary two-way ANOVA followed by a Dunnett post hoc test, and a pair Student's *t*-test were used for the statistical analyses of the different studies. The difference was considered significant when the *p-value was <0.05. Each data point represented the mean of three trials ± standard deviation in all experiments.

Supporting Information

Supporting Information is available from the Wiley Online Library or from the author.

Conflict of Interest

The authors declare no conflict of interest.

Data Availability Statement

The data that support the findings of this study are available from the corresponding author upon reasonable request.

[1] T. Jiang, G. Xu, G. Chen, Y. Zheng, B. He, Z. Gu, *Nano Res.* **2020**, *13*, 1810.

[2] M. B. Brown, A. C. Williams, *The Art and Science of Dermal Formulation Development*, Drugs and the Pharmaceutical Sciences, CRC Press, Boca Raton, FL **2019**.

[3] K. T. M. Tran, T. D. Gavitt, N. J. Farrell, E. J. Curry, A. B. Mara, A. Patel, L. Brown, S. Kilpatrick, R. Piotrowska, N. Mishra, S. M. Szczepanek, T. D. Nguyen, *Nat. Biomed. Eng.* **2021**, *5*, 998.

[4] T. Orenius, H. Säilä, K. Mikola, L. Ristolainen, *SAGE Open Nurs.* **2018**, *4*, 237796081875944.

[5] Y. Hao, W. Li, X. Zhou, F. Yang, Z. Qian, *J. Biomed. Nanotechnol.* **2017**, *13*, 1581.

[6] N. G. Rouphael, M. Paine, R. Mosley, S. Henry, D. V. McAllister, H. Kalluri, W. Pewin, P. M. Frew, T. Yu, N. J. Thornburg, S. Kabbani, L. Lai, E. V. Vassilieva, I. Skountzou, R. W. Compans, M. J. Mulligan, M. R. Prausnitz, A. Beck, S. Edupuganti, S. Heeke, C. Kelley, W. Nesheim, *Lancet* **2017**, *390*, 649.

[7] X. Zhou, Z. Luo, A. Baidya, H. Kim, C. Wang, X. Jiang, M. Qu, J. Zhu, L. Ren, F. Vajhadin, P. Tebon, N. Zhang, Y. Xue, Y. Feng, C. Xue, Y. Chen, K. Lee, J. Lee, S. Zhang, C. Xu, N. Ashammakhi, S. Ahadian, M. R. Dokmeci, Z. Gu, W. Sun, A. Khademhosseini, *Adv. Healthcare Mater.* **2020**, *9*, 2000527.

[8] R. F. Donnelly, K. Moffatt, A. Z. Alkilani, E. M. Vicente-Pérez, J. Barry, M. T. C. McCrudden, A. D. Woolfson, *Pharm. Res.* **2014**, *31*, 1989.

[9] R. F. Donnelly, T. R. R. Singh, M. J. Garland, K. Migalska, R. Majithiya, C. M. McCrudden, P. L. Kole, T. M. T. Mahmood, H. O. McCarthy, A. D. Woolfson, *Adv. Funct. Mater.* **2012**, *22*, 4879.

[10] G. Engelhardt, *Rheumatology* **1996**, *35*, 4.

[11] D. A. Castilla-Casadiego, H. Carlton, D. Gonzalez-Nino, K. A. Miranda-Muñoz, R. Daneshpour, D. Huitink, G. Prinz, J. Powell, L. Greenlee, J. Almodovar, *Mater. Sci. Eng., C* **2021**, *118*, 111544.

[12] L. K. Vora, P. R. Vavia, E. Larrañeta, S. E. J. Bell, R. F. Donnelly, *J. Interdiscip. Nanomed.* **2018**, *3*, 89.

[13] J. G. Turner, L. R. White, P. Estrela, H. S. Leese, *Macromol. Biosci.* **2021**, *21*, 2000307.

[14] B. Mbituyimana, G. Ma, Z. Shi, G. Yang, *Biomater. Adv.* **2022**, *142*, 213151.

[15] A. Panda, A. Shettar, P. K. Sharma, M. A. Repka, S. N. Murthy, *Int. J. Pharm.* **2021**, *593*, 120104.

[16] L. Liang, S. Zhang, G. A. Goenaga, X. Meng, T. A. Zawodzinski, A. J. Ragauskas, *Front. Chem.* **2020**, *8*, 570.

[17] J. Wang, Y. Ye, J. Yu, A. R. Kahkoska, X. Zhang, C. Wang, W. Sun, R. D. Corder, Z. Chen, S. A. Khan, J. B. Buse, Z. Gu, *ACS Nano* **2018**, *12*, 2466.

[18] W. Li, J. Y. Chen, R. N. Terry, J. Tang, A. Romanyuk, S. P. Schwendeman, M. R. Prausnitz, *J. Controlled Release* **2022**, *347*, 489.

[19] P. Kanaujia, P. Poovizhi, W. K. Ng, R. B. H. Tan, *Powder Technol.* **2015**, *285*, 2.

[20] J. P. Pezacki, J. A. Blake, D. C. Danielson, D. C. Kennedy, R. K. Lyn, R. Singaravelu, *Nat. Chem. Biol.* **2011**, *7*, 137.

[21] S. Henry, D. V. McAllister, M. G. Allen, M. R. Prausnitz, *J. Pharm. Sci.* **1998**, *87*, 922.

[22] E. Nagy, A. Andrásik, T. Smausz, T. Ajtai, F. Kun-Szabó, J. Kopniczky, Z. Bozóki, P. Szabó-Révész, R. Ambrus, B. Hopp, *Nanomaterials* **2021**, *11*, 996.

[23] H. Amani, M.-A. Shahbazi, C. D'Amico, F. Fontana, S. Abbaszadeh, H. A. Santos, *J. Controlled Release* **2021**, *330*, 185.

[24] A. Ripolin, J. Quinn, E. Larrañeta, E. M. Vicente-Perez, J. Barry, R. F. Donnelly, *Int. J. Pharm.* **2017**, *521*, 92.

[25] L. R. Pires, I. R. Amado, J. Gaspar, *Int. J. Pharm.* **2020**, *586*, 119590.

[26] J. Chen, W. Huang, Z. Huang, S. Liu, Y. Ye, Q. Li, M. Huang, *AAPS PharmSciTech* **2018**, *19*, 1141.

[27] A. J. Paredes, A. D. Permana, F. Volpe-Zanutto, M. N. Amir, L. K. Vora, I. A. Tekko, N. Akhavein, A. D. Weber, E. Larrañeta, R. F. Donnelly, *Mater. Des.* **2022**, *224*, 111416.

[28] "European Medicines Agency: EMEA/V/C/000033," https://www.ema.europa.eu/en/medicines/veterinary/EPAR/metacam (accessed: December 2022).

[29] A. J. Kreuder, J. F. Coetzee, L. W. Wulf, J. A. Schleining, B. KuKanich, L. L. Layman, P. J. Plummer, *BMC Vet. Res.* **2012**, *8*, 85.

[30] J. T. Jacon Freitas, O. M. M. Santos Viana, R. Bonfilio, A. C. Doriguetto, M. B. de Araújo, *Eur. J. Pharm. Sci.* **2017**, *109*, 347.

[31] D. Novakovic, J. Saarinen, T. Rojalin, O. Antikainen, S. J. Fraser-Miller, T. Laaksonen, L. Peltonen, A. Isomäki, C. J. Strachan, *Anal. Chem.* **2017**, *89*, 11460.

[32] "WORLD HEALTH ORGANIZATION Stability testing of active pharmaceutical ingredients and finished pharmaceutical products, WHO Technical report series, 2009, 953:87–123," https://database.ich.org/sites/default/files/Q1F_Stability_Guideline_WHO_2018.pdf (accessed: January 2023).

[33] S. Rojekar, L. K. Vora, I. A. Tekko, F. Volpe-Zanutto, H. O. McCarthy, P. R. Vavia, R. F. Donnelly, *Eur. J. Pharm. Biopharm.* **2021**, *165*, 41.